

Iron deposition influences the measurement of water diffusion tensor in the human brain: a combined analysis of diffusion and iron-induced phase changes

Xiaojun Xu¹ · Qidong Wang² · Jianhui Zhong^{3,4} · Minming Zhang¹

Received: 12 April 2015 / Accepted: 11 August 2015 / Published online: 26 August 2015
© Springer-Verlag Berlin Heidelberg 2015

Abstract

Introduction This study aims to evaluate the impact of iron deposition during aging on the measurement of water diffusion in the brain.

Methods Diffusion tensor images (DTI) and phase images collected from a group of healthy adults from 23 to 72 years old were retrospectively analyzed. The axial diffusivity, radial diffusivity, mean diffusivity (MD), and fractional anisotropy (FA) in the frontal white matter and deep gray matter nuclei were calculated. The phase changes in these regions were used to estimate local iron concentration. Pearson correlation analysis was used to evaluate the age dependence of DTI metrics and iron concentration. Multiple linear regression models were then built to examine the independent effect of age and iron deposition on DTI metrics.

Results Age-related iron deposition occurred in the putamen ($r=0.680$, $P<0.001$) and frontal white matter ($r=0.333$, $P=0.007$). In the putamen, FA increased with elevated iron concentration ($P=0.042$) excluding the effect of age, and MD decreased with iron deposition with marginal statistical significance ($P=0.067$). In the frontal white matter, increase in iron

level was also associated with a decrease in MD and an increase in FA. Moreover, radial diffusivity was more reduced than axial diffusivity as local iron concentration increased.

Conclusion Iron deposition in the brain during aging decreases water diffusion and increases the degree of anisotropy. Caution is needed when using DTI metrics for diagnosis of various neurological diseases involving abnormal iron deposition.

Keywords Brain iron · Brain aging · Diffusion tensor

Introduction

Diffusion tensor imaging (DTI) provides direct insight into microstructural properties of tissues through measurements of the magnitude and direction of water self diffusion [1, 2]. Two DTI metrics, mean diffusivity (MD), which describes the overall diffusivity, and fractional anisotropy (FA), which characterizes the degree of anisotropy, are most commonly used for delineating the characteristics of water diffusion. Any change in underlying structural features would probably result in a change in one or both of these DTI metrics.

It is well established that aging has a significant effect on water diffusion in the human brain. Typically, FA decreases while MD increases with advancing age in the white matter, commonly observed in regions such as the genu of the corpus callosum and the prefrontal lobe [3, 4], which are believed to be mostly due to increased diffusivity perpendicular to the direction of fibers [3, 4]. Generally, such change is considered as the result of age-related myelin breakdown [5]. By contrast, many authors reported increased FA and reduced MD in the deep gray matter during aging, especially in the putamen [6–11]. Further study [12] founded that eigenvalue λ_{23} showed an age-related decrease in the putamen, whereas the

✉ Xiaojun Xu
xxjmailbox@163.com

¹ Department of Radiology, Second Affiliated Hospital, Zhejiang University School of Medicine, 88 Jiefang Road, Hangzhou, Zhejiang Province, China 310009

² Department of Radiology, First Affiliated Hospital, Zhejiang University School of Medicine, Hangzhou, China

³ College of Biomedical Engineering and Instrument Science, Zhejiang University, Hangzhou, China

⁴ University of Rochester School of Medicine and Dentistry, Rochester, NY, USA

value of eigenvalue λ_1 was preserved during aging. This result indicated that increased FA and reduced MD during aging observed in the putamen might be a consequence of reduced diffusivity perpendicular to the direction of fibers. However, the underlying change of brain microstructure remains unclear.

Of the many changes accompanied aging is progressive iron deposition in the brain, notable especially in selective deep gray matter structures, such as the putamen [13–15]. Recently, high FA was found to be correlated with high iron concentration in the putamen [10]. Moreover, a significant increased FA was observed in the area with abnormal accumulation of iron content [16, 17]. Above studies suggested iron deposits in the brain may influence DTI metrics. Therefore, the change of water diffusion in the putamen during aging may not be a reflection of changes of underlying tissue microarchitecture, but of local iron accumulation.

In this study, we reanalyzed legacy MR data, which consisted of DTI and susceptibility weighted phase imaging (SWPI) data collected in a life span sample of healthy adults. The SWPI was used to estimate the brain iron concentration. The aim of this study was to evaluate the impact of iron deposition on the measurement of water diffusion in the brain.

Material and methods

Subjects

One hundred volunteers ranging from 20 to 80 years old were recruited from the local community and hospital staff to study the neuroradiological characterization of normal brain aging. The study was approved by the research ethics committee of the hospital. All the participants gave a written consent to participate in this study.

Sixteen subjects were excluded for the study due to abnormal appearance on the conventional T2-weighted images such as lacunar infarction and white matter hyperintensities. In the remaining 84 subjects, 7 subjects did not complete the DTI scanning due to discomfort and 6 subjects excluded for further analysis due to excessive motion artifact. In addition, six subjects did not perform the SWPI scanning due to technical reason. Therefore, DTI data were obtained from 71 subjects and SWPI data were obtained from 78 subjects. The results of DTI and SWPI were reported respectively elsewhere [12, 15].

In this study, the data of 65 subjects with both DTI and SWPI were retrospective analyzed. The study group included 35 men and 30 women ranging in age 23 to 72 years (mean=41.66, SD=13.65).

MR protocols

All the MR data were obtained using a 1.5-T scanner (Signa Excite II; GE Healthcare, Milwaukee, USA) with an eight-channel neurovascular phased array coil.

Conventional MR images were acquired and examined by an experienced neuroradiologist to exclude any morphologic abnormalities in the brain. The sagittal T2-weighted images were used to locate the precise positions of the anterior and posterior commissures. The following images were obtained parallel to the anterior-posterior commissural line as defined on the sagittal T2-weighted images.

A 3D gradient echo sequence (TR/TE=51/38 ms, flip angle=20, slice thickness=2 mm with no gap, slice number=28, FOV=24 cm, matrix size=256×256) was used for SWPI acquisition.

A single-shot spin-echo EPI sequence (TR/TE=10000/86 ms, slice thickness=3 mm with no gap, slice number=32, FOV=24 cm, matrix size=128×128, and NEX=2) was used for DTI acquisition. In addition to one non-diffusion-weighted image, diffusion-weighted images were acquired along 15 non-collinear directions with a b value of 1000 s/mm².

Image processing

Images were processed on a workstation from the manufacturer (Advantage Workstation 4.2, GE Healthcare, Milwaukee, USA).

The original SWPI images were filtered with a high-pass filter with a central matrix size of 32×32 to create the corrected phase image. The purpose of applying a high-pass filter was to remove slowly varying phase shifts, which arise predominantly from air-tissue interfaces and background field inhomogeneities. After filtering, the phase values measured on the corrected phase image are mainly induced by local iron deposition. Previous study demonstrated that the corrected phase value correlated negatively with the brain iron concentration [15]. The greater the negative phase value indicates higher brain iron concentration.

The original DTI images were first corrected to remove EPI distortions due to eddy currents, susceptibility, and motions by scaling, de-skewing, and translating methods. The diffusion tensor was then evaluated according to the Stejskal and Tanner equation on a voxel-by-voxel basis. Three pairs of eigenvalues ($\lambda_1, \lambda_2, \lambda_3$) and eigenvectors were obtained by the diagonalization of the tensor matrix. In the brain, λ_1 represents the water diffusivity parallel to the axonal fibers and is referred to as the axial diffusivity. Average of λ_2 and λ_3 is referred to as the radial diffusivity, which represents water diffusivity perpendicular to the axonal fibers. MD and FA values were defined as:

$$MD = (\lambda_1 + \lambda_2 + \lambda_3) / 3$$

$$FA = \sqrt{\frac{3(\lambda_1 - MD)^2 + (\lambda_2 - MD)^2 + (\lambda_3 - MD)^2}{2(\lambda_1^2 + \lambda_2^2 + \lambda_3^2)}}$$

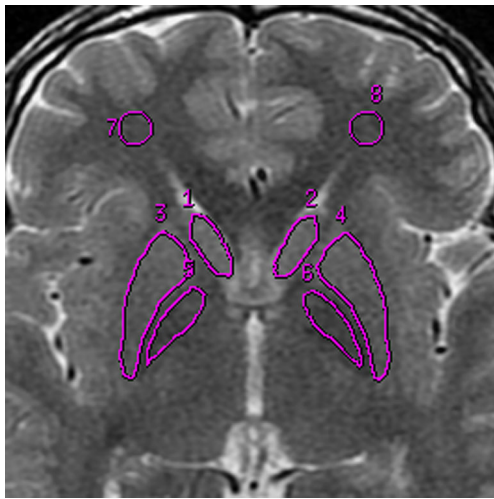


Fig. 1 ROIs depicted on the T2WI images. ROIs 1 and 2 correspond to the head of caudate, 3 and 4 to the putamen, 5 and 6 to the globus pallidus, and 7 and 8 to the bilateral frontal white matter

The corrected phase image and maps of diffusion metrics was co-registered to the T2-weighted image to bring different type of images located in the same space coordinates, so that the following region of interest (ROI)-based measurements can be derived from the same anatomical structures.

ROI-based analysis

We chose the frontal white matter (FWM) and several deep gray matter nuclei including the putamen, globus pallidus, and head of caudate nucleus as the ROI to access the relationship of iron deposition and water diffusion.

A trained neuroradiologist manually delineated the ROIs on the T2-weighted image through the anterior-posterior commissural line. The ROIs of the deep gray matter nuclei were drawn according to the anatomical structures, and for the FWM, circular ROIs with the size of 50 mm² were used (Fig. 1). The ROIs delineated on the T2-weighted image were replicated to the corrected phase image and maps of diffusion metrics of the same position to measure regional phase value, axial diffusivity, radial diffusivity, MD, and FA. The phase values were converted to iron concentration according to the equation proposed by Haccke et al.: 0.276 radians of phase to be equivalent to 60 µg Fe/g tissue [18].

Statistical analysis

Pearson correlation analysis was used first to test the age dependence of DTI metrics and iron concentration in each ROI. Multiple linear regression models were then built to examine the independent effect of age and iron deposition on DTI metrics. In this case, age and iron concentration were used as the explanatory variables, with DTI metrics as outcome variables. Variance inflation factor (VIF) was calculated to determine the collinearity of the age and iron concentration. The statistical analysis was performed with SPSS 16.0 (SPSS In., Chicago, IL) and the significant level was defined as the *P* value less than 0.05 by a two-tailed test.

Results

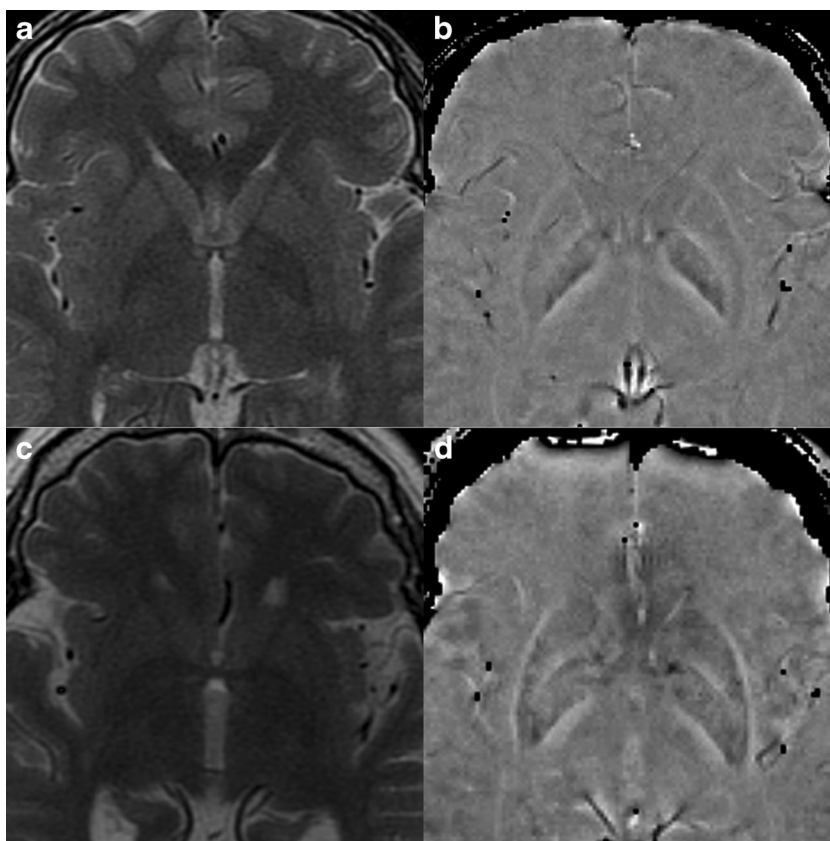
A comparison of typical MR images from young and old individuals was shown in Fig. 2. Deep gray matter structures of the elderly showed relative signal darkening on the T2-weighted image and corrected phase image, especially in the putamen. Signal loss in these structures was considered as the result of iron accumulation with aging [19]. Pearson correlation analysis showed the iron concentration in the putamen increased linearly with aging (Table 1; Fig. 3a). Besides, age-related iron deposition was detected in the FWM (Table 1; Fig. 3b). The change of iron concentration during aging in the head of caudate nucleus and globus pallidus did not reach the statistical significant level (Table 1, Fig. 3c, d). Thus, only the data from the putamen and FWM were further analyzed with multiple regression analysis to evaluate the impact of iron deposition and age on measurement of water diffusion in the brain.

Putamen: multiple regression analysis

Pearson correlation analysis showed that FA increased linearly with aging. Meanwhile, radial diffusivity and MD decreased, axial diffusivity tended to decrease with advancing age (Table 1, Fig. 4). The multiple linear regression analysis produced the following equations (Tables 2, 3):

$$\begin{aligned}
 \text{FA} &= 0.184 + (0.002 \times \text{Iron concentration; } \mu\text{g Fe/g tissue}) + (0.001 \times \text{Age; years})\text{MD} \\
 &= [6.787 + (-0.018 \times \text{Iron concentration; } \mu\text{g Fe/g tissue}) + (-0.004 \times \text{Age; years})] \times 10^{-4} \text{mm}^2/\text{sAxial diffusivity} \\
 &= [8.067 + (-0.010 \times \text{Iron concentration; } \mu\text{g Fe/g tissue}) + (-0.001 \times \text{Age; years})] \times 10^{-4} \text{mm}^2/\text{sRadial diffusivity} \\
 &= [6.162 + (-0.022 \times \text{Iron concentration; } \mu\text{g Fe/g tissue}) + (-0.006 \times \text{Age; years})] \times 10^{-4} \text{mm}^2/\text{s}
 \end{aligned}$$

Fig. 2 A comparison of MR image from young and old individuals. **a, c** T2-weighted images. **b, d** Corrected phase images. **a, b** Obtained from a 25-year-old man. **c, d** Obtained from a 65-year-old woman. All the images were through the anterior-posterior commissural line. Signal loss was apparent in the deep gray matter on the T2-weighted image and corrected phase image obtained from the old individual, especially the putamen



According to the equations above, local iron accumulation and aging were both associated with an increase of FA and reduction of water diffusivity in the putamen. The factors of age and iron concentration were found not collinearly related for VIF values < 10 . The statistically significant finding was that excluding the effect of age, FA increased with elevated iron concentration ($P=0.042$). In addition, radial diffusivity ($P=0.056$) and MD ($P=0.067$) were found decreased with elevated iron concentration with marginal statistical significance. Although these equations for FA, MD, and radial diffusivity accounted for only

18.3 %~26.5 % of the variance, nonetheless, the overall regression equations were highly significant. Above results indicated that local iron deposition would cause reduced water diffusivity and increased anisotropy in the putamen. Therefore, the physiologic iron deposition during aging may be the cause of increased FA and reduced MD observed in the putamen.

Frontal white matter: multiple regression analysis

Pearson correlation analysis showed FA decreased and radial diffusivity increased linearly with aging. Besides,

Table 1 Results of Pearson correlation analysis between iron concentration, DTI metrics, and age

	Iron concentration	Axial diffusivity	Radial diffusivity	Mean diffusivity (MD)	Fractional anisotropy (FA)
Putamen	<i>$r=0.680$</i> <i>$P<0.001$</i>	$r=-0.205$, $P=0.101$	<i>$r=-0.409$</i> <i>$P=0.001$</i>	<i>$r=-0.371$</i> <i>$P=0.002$</i>	<i>$r=0.463$</i> <i>$P<0.001$</i>
Globus pallidus	$r=-0.077$ $P=0.530$	$r=-0.085$ $P=0.501$	$r=-0.165$ $P=0.190$	$r=-0.146$, $P=0.247$	$r=0.212$ $P=0.091$
Caudate nucleus	$r=0.205$ $P=0.100$	<i>$r=-0.354$</i> <i>$P=0.004$</i>	<i>$r=-0.317$</i> <i>$P=0.010$</i>	<i>$r=-0.341$</i> <i>$P=0.005$</i>	$r=0.009$ $P=0.435$
Frontal white matter	<i>$r=0.333$</i> <i>$P=0.007$</i>	$r=-0.012$ $P=0.924$	$r=0.336$ <i>$P=0.006$</i>	$r=0.240$ $P=0.055$	$r=-0.342$ <i>$P=0.006$</i>

A P value of less than 0.05 was considered statistically significant and the corresponding results are shown in italics

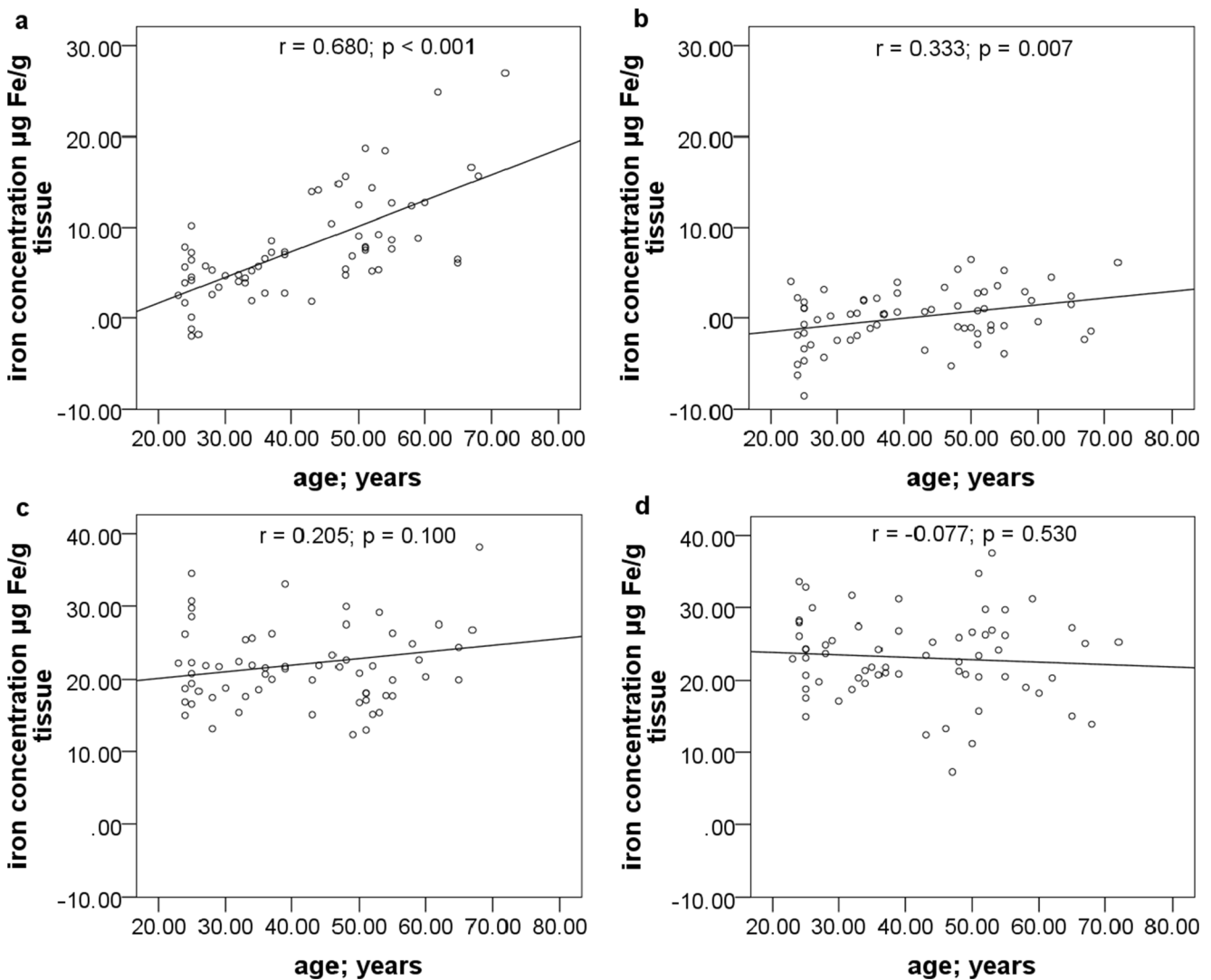


Fig. 3 The scatterplots of iron concentration with aging in the putamen (a), frontal white matter (b), head of caudate (c), and globus pallidus (d)

MD increased with advancing age with marginal statistical significance (Table 1, Fig. 5). The multiple linear

regression analysis produced the following equations (Tables 2 and 4):

$$FA = 0.408 + (0.004 \times \text{Iron concentration; } \mu\text{g Fe/g tissue}) + (-0.001 \times \text{Age; years})$$

$$MD = [6.752 + (-0.027 \times \text{Iron concentration; } \mu\text{g Fe/g tissue}) + (0.011 \times \text{Age; years})] \times 10^{-4} \text{ mm}^2/\text{s}$$

$$\text{Axial diffusivity} = [9.835 + (-0.014 \times \text{Iron concentration; } \mu\text{g Fe/g tissue}) + (0.000 \times \text{Age; years})] \times 10^{-4} \text{ mm}^2/\text{s}$$

$$\text{Radial diffusivity} = [5.211 + (-0.034 \times \text{Iron concentration; } \mu\text{g Fe/g tissue}) + (0.016 \times \text{Age; years})] \times 10^{-4} \text{ mm}^2/\text{s}$$

According to the equations above, the effect of iron deposition on DTI metrics was opposite to that of aging. Elevated iron concentration was associated with an increase of FA and a decrease of water diffusivity. Whereas, advanced age was associated with a decrease of FA and an increase of water diffusivity. The statistically significant finding was that removing the effect of iron deposition, FA decreased ($P=0.001$), radial

diffusivity ($P=0.002$) and MD ($P=0.025$) increased with advanced age. Another important finding was that FA increased with elevated iron concentration with marginal statistical significance ($P=0.065$). Above results indicate that aging is the main cause of the change of water diffusion we observed in the FWM, and also suggests that iron deposition in FWM may counteract the changes of water diffusivity induced by aging.

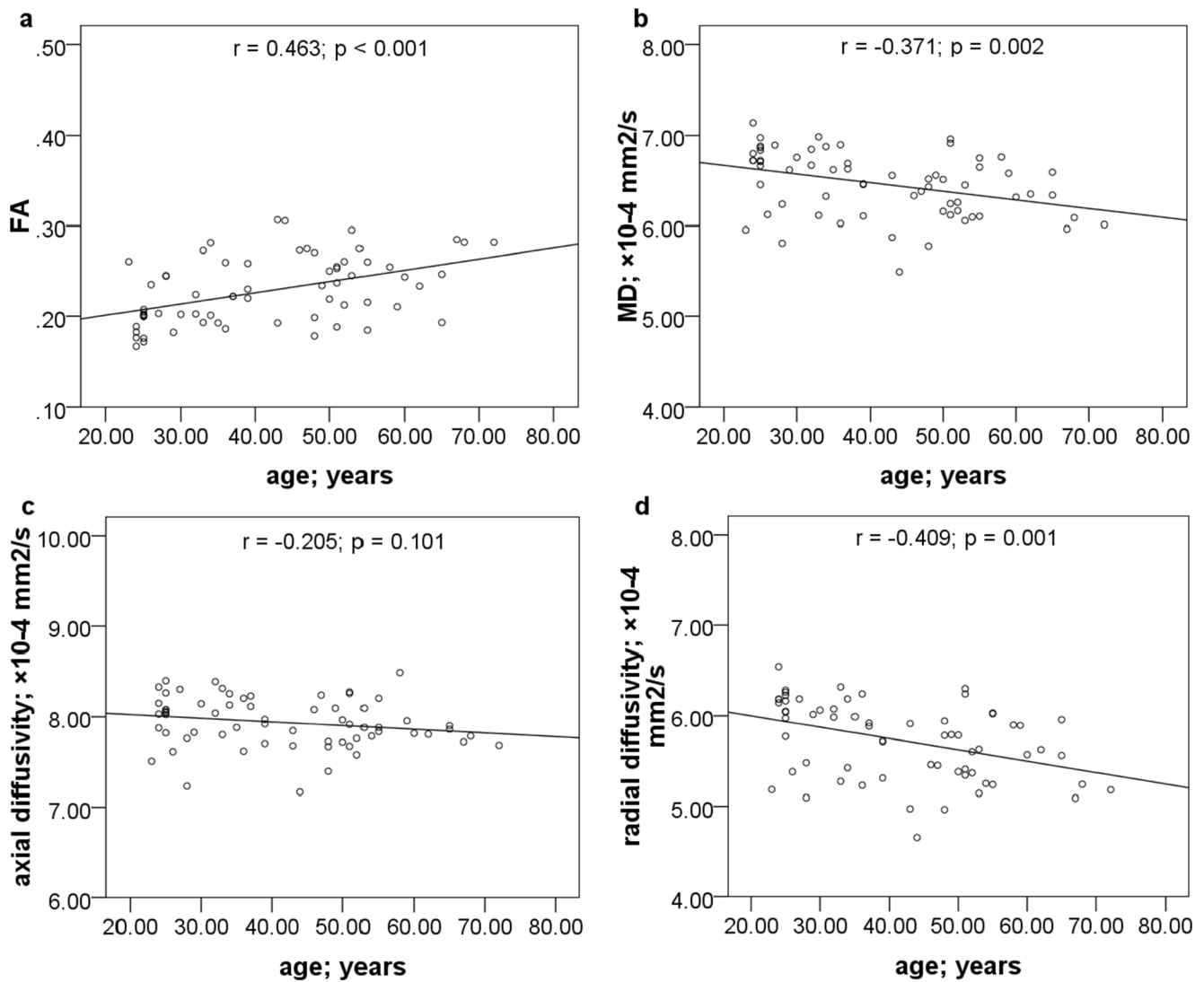


Fig. 4 The scatterplots of FA (a), MD (b), axial diffusivity (c), and radial diffusivity (d) with aging in the putamen

Discussion

In this study, we found that increased iron deposition would cause a decrease in the estimated diffusivity

and an increase in the estimated anisotropy. This finding indicates that iron deposition influences significantly the measurement of water diffusion tensor in the human brain.

Table 2 Results of multiple linear regression analysis: summary statistics

	Summary statistic	Outcome variable			
		Axial diffusivity	Radial diffusivity	Mean diffusivity (MD)	Fractional anisotropy (FA)
Putamen	R^2	0.065	<i>0.215</i>	<i>0.183</i>	<i>0.265</i>
	P of entire equation	0.126	<i>0.001</i>	<i>0.002</i>	<i>0.000</i>
	Variance inflation factor	1.861	1.861	1.861	1.861
Frontal white matter	R^2	0.004	<i>0.147</i>	0.084	<i>0.164</i>
	P of entire equation	0.874	<i>0.007</i>	0.066	<i>0.004</i>
	Variance inflation factor	1.125	1.125	1.125	1.125

A P value of less than 0.05 was considered statistically significant and the corresponding results are shown in italics

Table 3 Results of multiple linear regression analysis to examine the effect of age and iron on DTI metrics in the putamen

Explanatory variables	Outcome variable											
	Axial diffusivity			Radial diffusivity			Mean diffusivity (MD)			Fractional anisotropy (FA)		
	Coefficient	Standardized coefficient	<i>P</i>	Coefficient	Standardized coefficient	<i>P</i>	Coefficient	Standardized coefficient	<i>P</i>	Coefficient	Standardized coefficient	<i>P</i>
Intercept	8.067	–	0.000	6.162	–	0.000	6.787	–	0.000	0.184	–	0.000
Age	–0.001	–0.066	0.693	–0.006	–0.206	0.184	–0.004	–0.173	0.274	0.001	0.253	0.094
Iron	–0.010	–0.204	0.227	–0.022	–0.298	0.056	–0.018	–0.291	0.067	<i>0.002</i>	<i>0.308</i>	<i>0.042</i>

A *P* value of less than 0.05 was considered statistically significant and the corresponding results are shown in italics

The underlying mechanism of the reduced diffusivity may be related to the MR signal dephasing in magnetic inhomogeneities induced by local iron deposition. As a paramagnetic substance, iron deposited in the brain causes variations in magnetic susceptibility on a microscopic scale [20]. When

the brain is placed in an MR scanner, local field gradients are generated near these irons. The effect of these local gradients on the measurement of diffusion depends strongly on the scanning protocol. The conventional sequence, which is referred to as pulsed-gradient spin-echo (PGSE) sequence as we

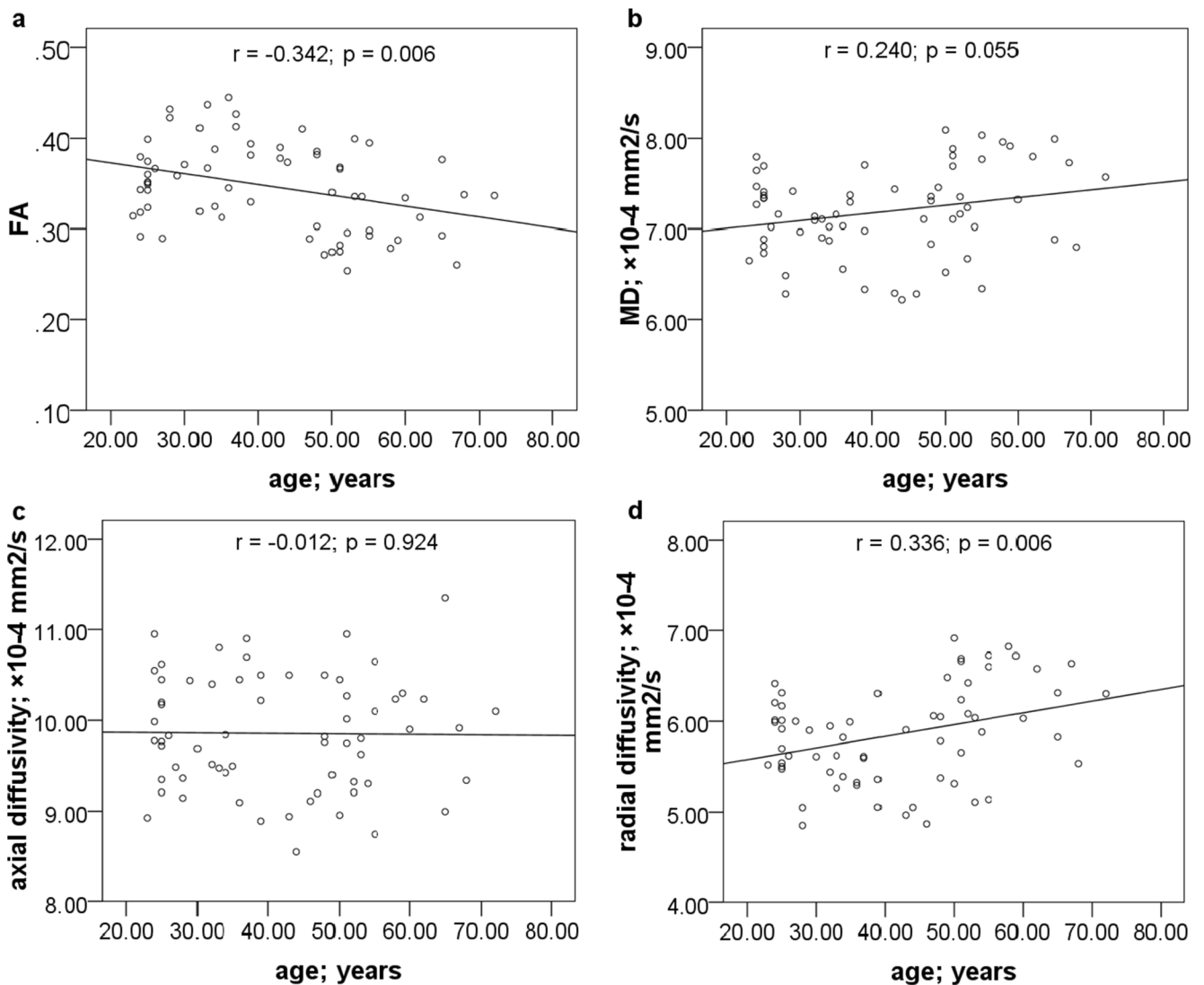


Fig. 5 The scatterplots of FA (a), MD (b), axial diffusivity (c), and radial diffusivity (d) with aging in the frontal white matter

Table 4 Results of multiple linear regression analysis to examine the effect of age and iron on DTI metrics in the frontal white matter

Explanatory variables	Outcome variable											
	Axial diffusivity			Radial diffusivity			Mean diffusivity (MD)			Fractional anisotropy (FA)		
	Coefficient	Standardized coefficient	<i>P</i>	Coefficient	Standardized coefficient	<i>P</i>	Coefficient	Standardized coefficient	<i>P</i>	Coefficient	Standardized coefficient	<i>P</i>
Intercept	9.835	–	0.000	5.211	–	0.000	6.752	–	0.000	0.408	–	0.00
Age	0.000	0.011	0.937	<i>0.016</i>	<i>0.402</i>	<i>0.002</i>	<i>0.011</i>	<i>0.297</i>	<i>0.025</i>	<i>–0.001</i>	<i>–0.419</i>	<i>0.001</i>
Iron	–0.014	–0.069	0.612	–0.034	–0.196	0.120	–0.027	–0.173	0.186	0.004	0.231	0.065

A *P* value of less than 0.05 was considered statistically significant and the corresponding results are shown in italics

used in this study, is sensitive to these self-induced internal gradients [21]. Zhong and colleagues developed a simple theoretical model to describe the effect of susceptibility variations on the measured water diffusivity [22, 23]. They showed that the measured apparent diffusion coefficient (ADC, which is equivalent to the MD value used above) could be described as a weighted sum of ADCs from individual magnetic isochromats. Even though some isochromats will have enhanced diffusion effects while others reduced diffusion effects when compared to the case without such local gradient, for local gradients symmetrically distributed with zero mean as described by a Gaussian distribution, the isochromats with reduced ADC have a higher signal than those with increased ADC. The higher weighting of the attenuated signal for isochromats with reduced ADC resulted in a reduced overall ADC. In other words, this apparently counterintuitive ADC decrease can be explained by the nonlinear relationship between the diffusion signal attenuation with the *b* value: negative interactions between the local gradients induced by iron oxide particles and the applied diffusion-weighting gradients contribute more to increase the signal level (or a decrease in local effective *b* value) than positive interactions contribute to decrease the signal level (or an increase in local effective *b* values). The phenomenon of reduced apparent diffusion was experimentally confirmed in heterogeneous media containing superparamagnetic iron oxide particles of varying concentrations [23]. A further study demonstrated that ADC was also reduced in rat brain due to intravascular susceptibility variations induced by injection of the superparamagnetic intravascular contrast agent [24]. Our current results for human brains provided the evidence that magnetic susceptibility variations due to the physiologic iron deposition during aging would result in a similar reduction of measured water diffusivity.

All the above studies indicate inhomogeneous sample susceptibility influences water diffusion measurements. However, this conclusion is contradictory to some other reports [25, 26]. These authors measured ADC changes in various excited nerves with their axis aligned longitudinally along or perpendicular to the static field B_0 . Changes in sample orientation would maximize the change in the magnitude

of susceptibility-induced gradients. In addition, ADC measured with PGSE sequence was compared with that using the sequence insensitive to the internal field gradients. They found that the measured ADC was independent of sample orientation and was unaffected by the scanning sequence. Furthermore, an *in vivo* study demonstrated that the measured ADC was unaffected by the presence of known susceptibility-induced gradients at the interface between the petrous bone and brain parenchyma [27]. There may be several possibilities to account for the discrepancy between different studies, but we believe that it is most likely that background gradients induced through the susceptibility difference of various interface are of macroscopic in nature, whereas the gradients induced by iron deposition are microscopic and are in such a scale that the whole field distribution described by a Gaussian function can be sampled within the diffusion time set by the pulse sequence. The effect of susceptibility-induced gradients on water diffusion measurements is likely very dependent on macroscopic or microscopic natures and detailed distributions of local susceptibility variation centers.

Effects of the local gradients on the measured diffusion anisotropy depend on not only the general distribution of the local field but also specific geometry of the susceptibility sources and surrounding tissue arrangements. Some recent studies suggest that magnetic susceptibility in the brain is itself a tensor quantity [28, 29]. A quantitative model to explain the increase FA as we observed may be related to this phenomenon but is beyond the scope of the current work. However, the observed increase in anisotropy is at least partially related to the MR signal dephasing due to local iron deposition, which leads to a decrease in local signal-to-noise ratio (SNR). Previous studies have showed that anisotropy measures are susceptible to noise contamination [30, 31]. Image noise produces a random perturbation of the diffusion tensor. In anisotropic systems, the value of the largest eigenvalue is overestimated and the lowest eigenvalue underestimated [30, 31]. Therefore, lower SNR makes anisotropic structures appear more anisotropic. Moreover, the degree of diffusion anisotropy increases as SNR decreases [30]. Hence, it is reasonable to expect an apparent higher FA in the iron-rich

brain region. In our study, radial diffusivity seemed to be more restricted than axial diffusivity as local iron concentration increased. We believe that it is the result of a combined action of susceptibility-induced gradients on water diffusion and lower SNR on anisotropy measurement. Further study is clearly needed to clarify the relative impact of these two factors on FA measurement.

In spite of the above-mentioned complications and ambiguity, our result suggests unambiguously that iron deposition affects significantly the measurements of water diffusion in the brain. This finding is important because it indicates that iron deposition in the brain would complicate the interpretation of single measurements of water diffusion. In addition to aging, the accumulation of iron in the brain also occurs, for example, in hemorrhage [32] and neural degenerative diseases [33]. Recently, several authors reported their initial results with measurements of water diffusion through DTI technique to explore the underlying microscopic structural features of the brain with neural degenerative diseases [34–37]. Due to excessive iron deposition in the brain with such diseases, the intrinsic susceptibility variations may be more serious than normal brain. Moreover, susceptibility variations rise considerably with increasing field strength [38]. Therefore, the influence of local iron deposition on diffusion measurements must be taken into consideration in interpretation of diffusion data, especially for the experimental and clinical studies on high field MR scanners.

The main limitation of this study was that there was no gold standard for a precise determination of regional brain iron concentration. In our study, brain iron concentration was estimated using SWPI through the effect of iron on brain tissue susceptibility. Although it is influenced by heme iron and other non-iron source such as the application of high-pass filter, the phase image has been recognized as a reliable estimate of local iron concentration by many studies [15, 18, 39–42]. Recently, a new approach that uses the phase from SWI data called quantitative susceptibility mapping (QSM) provides a practical way to quantify the iron content [43]. It is commonly assumed that paramagnetic iron is the predominant source of susceptibility variations in gray matter and can be assessed with QSM. In future work, QSM may be used to accurately measure brain iron content. One additional limitation was that we did not set up a brain area which was not affected by iron deposition as a reference area to determine the effect of iron deposition on the DTI metrics. However, the brain has physiological iron deposition during aging. It is impossible to find a brain region that is not affected by age-related iron deposition. Phantom study is needed to further clarify the effect of iron deposition on the DTI metrics.

In conclusion, our study demonstrates that brain iron deposition influences the measurements of water diffusion. Caution is needed in use of DTI metrics for diagnosis of various neurological diseases involving abnormal iron or other paramagnetic substances deposition, particularly at higher fields.

Acknowledgments This work was supported by the National Key Technology R&D Program of China (2012BAI10B04), the National Natural Science Foundation of China (81371519), the Zhejiang Provincial Natural Science Foundation of China (LY12H18002), the Medical Scientific Research Foundation of Zhejiang Province (2009QN005), and the Educational Scientific Research Foundation of Zhejiang Province (Y200909841).

Ethical standards and patient consent We declare that all human studies have been approved by the Research Ethics Committee of Second Affiliated Hospital, Zhejiang University School of Medicine, and have therefore been performed in accordance with the ethical standards laid down in the 1964 Declaration of Helsinki and its later amendments. We declare that all patients gave informed consent prior to inclusion in this study.

Conflict of interest We declare that we have no conflict of interest.

References

1. Le Bihan D, Mangin JF, Poupon C et al (2001) Diffusion tensor imaging: concepts and applications. *J Magn Reson Imaging* 13: 534–546
2. Sundgren PC, Dong Q, Gómez-Hassan D, Mukherji SK, Maly P, Welsh R (2004) Diffusion tensor imaging of the brain: review of clinical applications. *Neuroradiology* 46:339–350
3. Sullivan EV, Pfefferbaum A (2006) Diffusion tensor imaging and aging. *Neurosci Biobehav Rev* 30:749–761
4. Sullivan EV, Pfefferbaum A (2007) Neuroradiological characterization of normal adult ageing. *Br J Radiol* 80:S99–S108
5. Song SK, Yoshino J, Le TQ et al (2005) Demyelination increases radial diffusivity in corpus callosum of mouse brain. *NeuroImage* 15(26):132–140
6. Bhagat YA, Beaulieu C (2004) Diffusion anisotropy in subcortical white matter and cortical gray matter: changes with aging and the role of CSF-suppression. *J Magn Reson Imaging* 20:216–227
7. Furutani K, Harada M, Minato M, Morita N, Nishitani H (2005) Regional changes of fractional anisotropy with normal aging using statistical parametric mapping (SPM). *J Med Investig* 52:186–190
8. Zhang YT, Zhang CY, Zhang J, Li W (2005) Age related changes of normal adult brain structure: analyzed with diffusion tensor imaging. *Chin Med J* 118:1059–1065
9. Abe O, Yamasue H, Aoki S et al (2008) Aging in the CNS: comparison of gray/white matter volume and diffusion tensor data. *Neurobiol Aging* 29:102–116
10. Pfefferbaum A, Adalsteinsson E, Rohlfing T, Sullivan EV (2010) Diffusion tensor imaging of deep gray matter brain structures: effects of age and iron concentration. *Neurobiol Aging* 31:482–493
11. Pal D, Trivedi R, Saksena S et al (2011) Quantification of age and gender related changes in diffusion tensor imaging indices in deep grey matter of the normal human brain. *J Clin Neurosci* 18:193–196
12. Wang Q, Xu X, Zhang M (2010) Normal aging in the basal ganglia evaluated by eigenvalues of diffusion tensor imaging. *AJNR Am J Neuroradiol* 31:516–520

13. Hallgren B, Sourander P (1958) The effect of age on the non-haemin iron in the human brain. *J Neurochem* 3:41–51
14. Schipper HM (2004) Brain iron deposition and the free radical-mitochondrial theory of ageing. *Ageing Res Rev* 3:265–301
15. Xu X, Wang Q, Zhang M (2008) Age, gender, and hemispheric differences in iron deposition in the human brain: an in vivo MRI study. *NeuroImage* 40:35–42
16. Awasthi R, Gupta RK, Trivedi R, Singh JK, Paliwal VK, Rathore RK (2010) Diffusion tensor MR imaging in children with pantothenate kinase associated neurodegeneration with brain iron accumulation and their siblings. *AJNR Am J Neuroradiol* 31:442–447
17. Ling HW, Ding B, Wang H, Zhang H, Chen KM (2011) Could iron accumulation be a etiology of the white matter change in Alzheimer's disease: using phase imaging to detect white matter iron deposition based on diffusion tensor imaging. *Dement Geriatr Cogn Disord* 31:300–308
18. Haacke EM, Muhammad A, Khan A et al (2007) Establishing a baseline phase behavior in magnetic resonance imaging to determine normal vs. abnormal iron content in the brain. *J Magn Reson Imaging* 26:256–264
19. Drayer B, Burger P, Darwin R, Riederer S, Herfkens R, Johnson GA (1986) MRI of brain iron. *AJR Am J Roentgenol* 147:103–110
20. Haacke EM, Cheng NY, House MJ et al (2005) Imaging iron stores in the brain using magnetic resonance imaging. *Magn Reson Imaging* 23:1–25
21. Hong X, Dixon TW (1992) Measuring diffusion in inhomogeneous systems in imaging mode using antisymmetric sensitizing gradients. *J Magn Reson* 99:561–570
22. Zhong J, Gore JC (1991) Studies of restricted diffusion in heterogeneous media containing variations in susceptibility. *Magn Reson Med* 19:276–284
23. Zhong J, Kennan RP, Gore JC (1991) Effects of susceptibility variations on NMR measurement of diffusion. *J Magn Reson* 95:267–280
24. Dose MD, Zhong J, Gore JC (1999) In vivo measurement of ADC change due to intravascular susceptibility variation. *Magn Reson Med* 41:236–240
25. Trudeau JD, Thomas DW, Hawkins J (1995) The effect of inhomogeneous sample susceptibility on measured diffusion anisotropy using NMR imaging. *J Magn Reson B* 108:22–30
26. Beaulieu C, Allen PS (1996) An in vitro evaluation of the effects of local magnetic susceptibility induced gradients on anisotropic water diffusion in nerve. *Magn Reson Med* 36:39–44
27. Clark CA, Barker GJ, Tofts PS (1999) An in vivo evaluation of the effects of local magnetic susceptibility-induced gradients on water diffusion measurements in human brain. *J Magn Reson* 141:52–61
28. Liu C, Li W, Wu B, Jiang Y, Johnson GA (2012) 3D fiber tractography with susceptibility tensor imaging. *NeuroImage* 59:1290–1298
29. Li W, Wu B, Avram AV, Liu C (2012) Magnetic susceptibility anisotropy of human brain in vivo and its molecular underpinnings. *NeuroImage* 59:2088–2097
30. Pierpaoli C, Basser PJ (1996) Toward a quantitative assessment of diffusion anisotropy. *Magn Reson Med* 36:893–906
31. Anderson AW (2001) Theoretical analysis of the effects of noise on diffusion tensor imaging. *Magn Reson Med* 46:1174–1188
32. Haris M, Gupta RK, Husain N, Hasan KM, Husain M, Narayana PA (2006) Measurement of DTI metrics in hemorrhagic brain lesions: possible implication in MRI interpretation. *J Magn Reson Imaging* 24:1259–1268
33. Zecca L, Youdim MB, Riederer P, Cormor JR, Crichton RR (2004) Iron, brain ageing and neurodegenerative disorders. *Nat Rev Neurosci* 5:863–873
34. Yoshikawa K, Nakata Y, Yamada K, Nakagawa M (2004) Early pathological changes in the parkinsonian brain demonstrated by diffusion tensor MRI. *J Neurol Neurosurg Psychiatry* 75:481–484
35. Boska MD, Hasan KM, Kibuule D et al (2007) Quantitative diffusion tensor imaging detects dopaminergic neuronal degeneration in a murine model of Parkinson's disease. *Neurobiol Dis* 26:590–596
36. Vaillancourt DE, Spraker MB, Prodoehl J et al (2009) High-resolution diffusion tensor imaging in the substantia nigra of de novo Parkinson disease. *Neurology* 72:1378–1384
37. Kantarci K, Avula R, Senjem ML et al (2010) Dementia with Lewy bodies and Alzheimer disease: neurodegenerative patterns characterized by DTI. *Neurology* 74:1814–1821
38. Rossi C, Boss A, Martirosian P et al (2008) Influence of steady background gradients on the accuracy of molecular diffusion anisotropy measurements. *Magn Reson Imaging* 26:1250–1258
39. Zhu WZ, Zhong WD, Wang W et al (2009) Quantitative MR phase-corrected imaging to investigate increased brain iron deposition of patients with Alzheimer disease. *Radiology* 253:497–504
40. Zhang J, Zhang Y, Wang J et al (2010) Characterizing iron deposition in Parkinson's disease using susceptibility-weighted imaging: an in vivo MR study. *Brain Res* 1330:124–130
41. Jin L, Wang J, Zhao L et al (2011) Decreased serum ceruloplasmin levels characteristically aggravate nigral iron deposition in Parkinson's disease. *Brain* 134:50–58
42. Zivadinov R, Heininen-Brown M, Schirda CV et al (2012) Abnormal subcortical deep-gray matter susceptibility-weighted imaging filtered phase measurements in patients with multiple sclerosis: a case-control study. *Neuroimage* 59:331–339
43. Liu C, Li W, Tong KA et al (2015) Susceptibility-weighted imaging and quantitative susceptibility mapping in the brain. *J Magn Reson Imaging* 42:23–41